A sensitivity study on the Dense Shelf Water formation in the Okhotsk Sea

You-ichiro Sasajima[1], Hiroyasu Hasumi[1] and Tomohiro Nakamura[2]

[1] Center for Climate System Research, University of Tokyo, Chiba, Japan
E-mail address: sasajima@ccsr.u-tokyo.ac.jp
[2] Institute of Low Temperature Science, Hokkaido University, Sapporo, Japan

Introduction

The Okhotsk Sea (Fig. 1) is believed to be the main source of North Pacific Intermediate Water (NPIW; *e.g.*, Talley, 1991; Yasuda *et al.*, 1997). The source water of the NPIW in the Okhotsk Sea is called the Okhotsk Sea Mode Water (OSMW) and is characterized by a minimum of potential vorticity whose density range is 26.6–27 σ_θ (Yasuda, 1997). The OSMW is formed by the mixing of the Dense Shelf Water (DSW), the Western Subarctic Water from the North Pacific through the Kuril Straits (Kitani, 1973), and the Forerunner of the Soya Warm Current Water from the Japan Sea through the Soya Strait (Takizawa, 1982; Watanabe and Wakatsuchi, 1998).

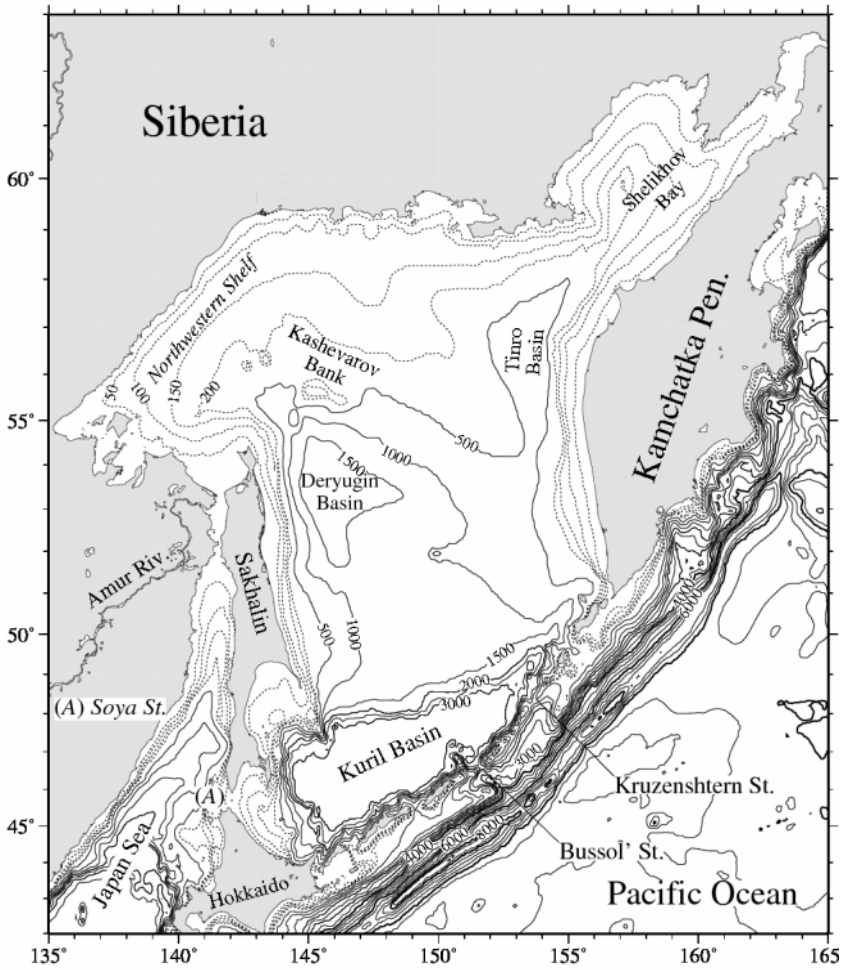

Fig. 1 Map of the Okhotsk Sea with bottom topography (in m).

The DSW is relatively cold and fresh water in the Okhotsk Sea. Its density range is within 26.6−27.05 σ_θ, although definitions of the range are slightly different among studies. Itoh *et al.* (2003) estimated the mixing ratio of the three types of water masses to form the OSMW from an isopycnal climatological dataset based on historical observations and suggested that nearly half of the OSMW consists of the DSW.

Kitani (1973) suggested that the DSW, with density up to 27.02 σ_θ, is formed by brine rejection through a high sea ice formation in the northwestern shelf region located northwest of Sakhalin (see Fig. 1). A high production of ice takes place in the coastal polynya along the northwestern coast of the Okhotsk Sea because of strong offshore winds and cold air temperature in winter, then it is considered that the brine rejection to form the DSW mainly occurs in that region (Alfultis and Martin, 1987; Martin *et al.*, 1998; Ohshima *et al.*, 2003; Shcherbina *et al.*, 2003). The formed DSW is transported to the south along the eastern coast of Sakhalin by the East Sakhalin Current (Ohshima *et al.*, 2002; Mizuta *et al.*, 2003) and contributes to the OSMW formation.

Impacts of factors leading to the DSW formation have been demonstrated by some numerical studies. Nakamura *et al.* (2006) investigated the effect of tidal mixing in the Kuril Straits for the DSW formation with a sea–ice coupled model. They simulated ocean circulations with and without the tidal mixing effect which is represented by setting a strong vertical diffusivity around the Kuril Islands and suggested that more DSW is formed by the tidal mixing effect through the following process. An upward salinity flux to the upper layer occurs due to the tidal mixing effect around the Kuril Islands and increases salinity in the upper layer. This positive anomaly of salinity by tidal mixing is transported from the Kuril Islands to the north through the eastern part of the Okhotsk Sea by a basin-scale cyclonic circulation which is mainly driven by wind stress (Ohshima *et al.*, 2004). As more saline (denser) brine is rejected in the northwestern shelf region because of the transported positive salinity anomaly, more DSW is formed.

Matsuda (2008) examined the impact of wind strength on the DSW formation with the tidal mixing effect, and showed that stronger winds also increase the DSW production. He explained that the wind-driven cyclonic circulation intensified by the amplified wind transports the more positive salinity anomaly originating with the tidal mixing effect to the northwestern shelf region. This transported salinity anomaly results in more saline (denser) brine and more DSW formation than those with the tidal mixing effect only. As mentioned later, it seems that the amplified wind has more effect on DSW formation.

However, the horizontal resolutions of the models are 1° in Nakamura *et al.* (2006) and a half degree in Matsuda (2008). These horizontal resolutions are too coarse to resolve well the northwestern coastal polynya which is several tens of kilometers in width (Martin *et al.*, 1998). Then, it is suggested that the DSW formation in the northwestern coastal polynya has not been well reproduced in former studies. In this study, the impacts of factors leading to the DSW formation are examined using a sea−ice coupled model with a horizontal resolution which is several kilometers in the northern part of the Okhotsk Sea. It is then expected that the model will resolve the coastal polynya along the northwestern coast.

Model Configuration

Numerical model

The Center for Climate System Research (CCSR) Ocean Component Model version 4.2 (COCO4.2; *e.g.*, Hasumi, 2006) is employed as the ice–ocean coupled model in this study. COCO4.2 solves primitive equations for three-dimensional ocean circulation and sea ice formation in the generalized curvilinear horizontal coordinate. By virtue of this coordinate system, one can arrange a computational grid pattern with locally high horizontal resolution and efficiently simulate phenomena on a small scale and their interaction with a circulation field in the relatively extensive surrounding area under a limitation of computational resources.

Figure 2a shows the model domain and the computational grid pattern in this study. The model domain covers the North Pacific. The horizontal resolution is up to 790 km in the South Pacific while it is less than 8 km in the northern part of the Okhotsk Sea to well resolve the northwestern coastal polynya and brine rejection (Fig. 2b).

The model topography is basically made from Earth Topography-5 Minute (ETOPO5; National Geophysical Data Center, 1988). The topography

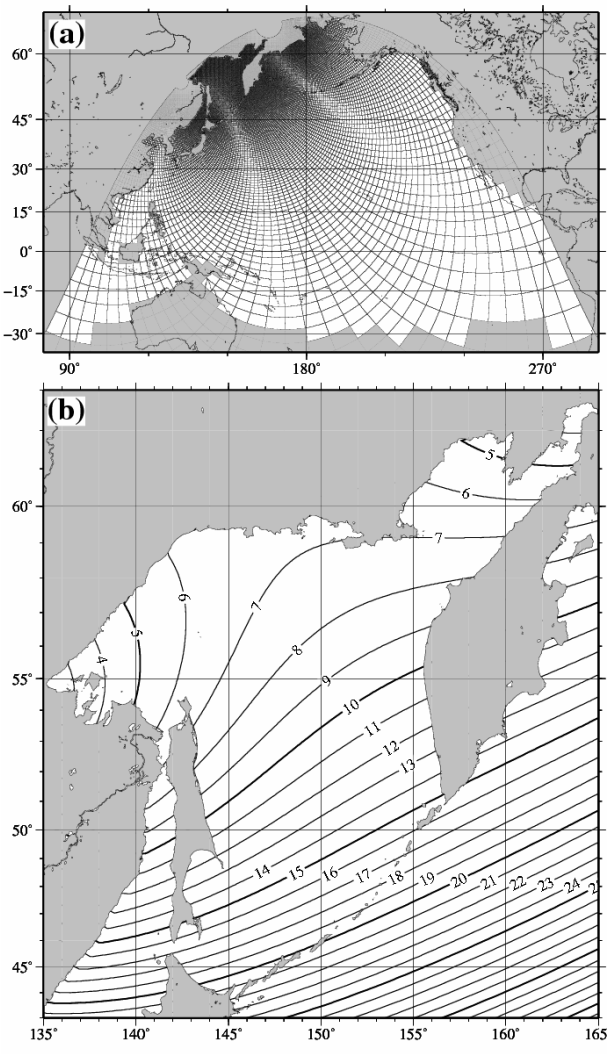

Fig. 2 (a) Computational grid pattern of the model in this study. The model calculates the ocean circulation and the sea ice formation in the white region. (b) Horizontal resolution of the model around the Okhotsk Sea (in km).

data made by Ono *et al.* (2006) is also used around the Kashevarov Bank because of inaccuracy of the ETOPO5 data in that region.

Boundary conditions

Simulated temperature and salinity are restored to the Polar Science Center Hydrographic Climatology (PHC; Steel *et al.*, 2001) from 15°S to the south. Sea surface salinity (SSS) is also restored to the PHC while it is not restored in the Okhotsk Sea in order to examine the salinity transport at the upper layer, as mentioned in Nakamura *et al.* (2006) and Matsuda (2008).

The experiments in this study are shown in Table 1. In all the experiments, the sea surface momentum and heat fluxes are calculated basically from the monthly climatological dataset of the Ocean Model Intercomparison Project (OMIP; Röske, 2001), which is based on European Centre for Medium-Range Weather Forecasts (ECMWF) 15-year reanalysis. The bulk formulae of Kara *et al.* (2000) are used for the flux calculation from the OMIP data. The OMIP dataset is directly applied in Run 1 and Run 2.

The vertical mixing effect by the tide in the Kuril Straits is implemented in Run 2, Run 3 and Run 4. The background vertical diffusivity coefficient is set to 200 $cm^2\ s^{-1}$ over the sill around the Kuril Islands in these experiments to represent the vertical mixing effect while it is less than 3 $cm^2\ s^{-1}$ (Tsujino *et al.*, 2000) in the other region. Nakamura *et al.* (2006) adopted the value of 200 $cm^2\ s^{-1}$ in their model, based on the results of former studies (Nakamura *et al.*, 2000; Nakamura and Awaji, 2004). Results of Matsuda (2008) also supported the validity of this value in terms of the DSW formation and its transport.

Ohshima *et al.* (2003) pointed out that the wind speed data reanalyzed by ECMWF are smaller than those of observed *in-situ* data, by about 25% in the Okhotsk Sea. Some numerical studies for the Okhotsk Sea have adopted the ECMWF wind stress amplified by factors of about 1.5 (*e.g.*, Simizu and Ohshima, 2002; Simizu and Ohshima, 2006). The wind stress of ECMWF is also used in Matsuda (2008), and he reported that a realistic circulation on the isopycnal surface of 26.8 σ_θ is reproduced with the amplified wind stress by a factor of 1.5. The wind stress of the OMIP data is also amplified by a factor of 1.5 in the Okhotsk Sea in Run 3 and Run 4.

Table 1 List of experiments.

Simulation	Description
Run 1	Directly driven by the OMIP data set.
Run 2	Run 1 with tidal mixing effect around the Kuril Islands.
Run 3	Run 2 with wind stress amplified by a factor of 1.5 in the Okhotsk Sea.
Run 4	Run 3 with removing river runoffs in the Okhotsk Sea, excluding the Amur river.

Figure 3 shows a comparison of river runoff in the Okhotsk Sea between the OMIP dataset and that from *in-situ* observation (Perry *et al.*, 1996). The river runoff of the OMIP is calculated by a land model using the ECMWF evaporation and precipitation data. The annual mean river runoff of the Amur River is about 10,000 $m^3 s^{-1}$ in the two datasets. On the other hand, the total amount of annual mean river runoffs in the Okhotsk Sea, excluding the Amur River, is 6,644 $m^3 s^{-1}$ in the OMIP data while it is 2,205 $m^3 s^{-1}$ in Perry *et al.* (1996). Results of SSS in Run 1, Run 2 and Run 3 (Figs. 4a, b and c), in which the OMIP river runoff data are directly used, show strong low-salinity fronts along the northwestern coast where the DSW is mainly formed. River runoffs in the Okhotsk Sea, except the Amur River, are removed in Run 4 in order to examine the impact of the uncertainty of river runoff among datasets to the DSW formation.

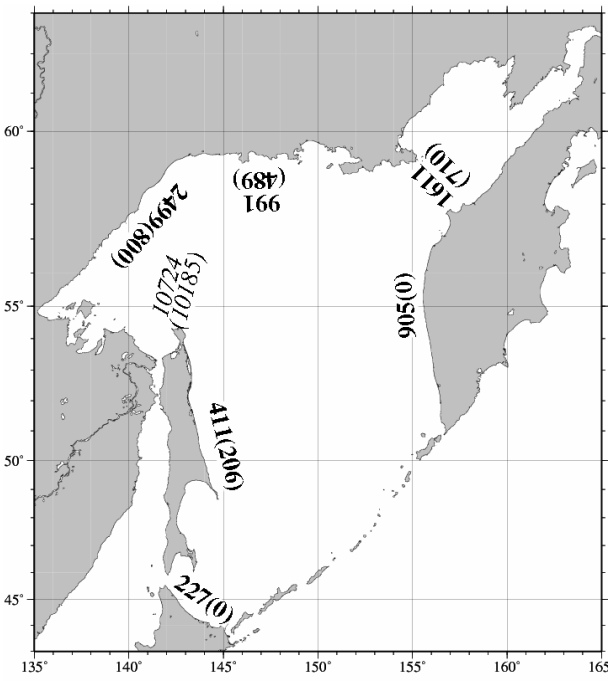

Fig. 3 Bracketed figures denote the annual mean runoffs from Perry *et al.* (1996) while those without brackets are values of the OMIP dataset along same coast (in $m^3 s^{-1}$). Figures in bold indicate, in clockwise order from the southwest, the runoffs along the northeastern coast of Hokkaido, the eastern coast of Sakhalin, the northwestern coast of the Okhotsk Sea, the northern coast of the Okhotsk Sea, the Shelikov Bay, and the western coast of the Kamchatka Peninsula while those in italics indicate the annual mean runoff of the Amur River.

In each experiment, the model is integrated for 16 model years from a static state with the temperature and salinity fields in January of the PHC. The sea ice formation, sea surface salinity and the DSW formation reach a steady state in the Okhotsk Sea. Results of the experiments in the 16th model year are compared in this study.

Results

Table 2 shows the production rate of the DSW in each experiment. Definition of the DSW production rate is based on Itoh *et al.* (2003). They defined the DSW as water on the northwestern shelf, with density within 26.75–27.05 σ_θ, temperature less than 0°C and its production rate as the total volume of DSW existing from spring to summer divided by a year. In this study, the DSW production rate is defined as the volume of the DSW existing from April to September in an area north of 54°N and west of 153°E, with the bottom depth shallower than 200 m divided by a year.

The DSW production rate by Run 1 is smaller than the range of estimates based on observations (Martin *et al.*, 1998; Gladyshev *et al.*, 2000; Itoh *et al.*, 2003). The DSW production increases on adding the effects of the tide around the Kuril Islands, the intensification of the wind stress and removing the runoffs in Run 2, Run 3 and Run 4, respectively, and is within the range of the observational estimates. DSW production rates in Run 2, Run 3 and Run 4 are clearly larger than those in the experiment with the vertical diffusion coefficient of 200 $cm^2 s^{-1}$ around the Kuril Islands in Nakamura *et al.* (2006). Even the production rate in Run 1, in which the tidal effect is not implemented, is slightly larger than that in the experiment in Nakamura *et al.* (2006). The annual sea ice production in the Okhotsk Sea in each experiment (Table 3) is much larger than that in the experiment in Nakamura *et al.* (2006) and close to that estimated from observed data (*e.g.*, Ohshima *et al.*, 2003). Figure 5 shows the horizontal distributions of annual sea ice production in the northwestern shelf region. The coastal polynya is clearly reproduced along the northwestern coast in each experiment because of the much higher resolution than that in Nakamura *et al.* (2006), as mentioned in the previous sections. The model in each experiment, then, also reproduced the high sea ice production in the coastal polynya mentioned in the observational studies (Alfultis and Martin, 1987;

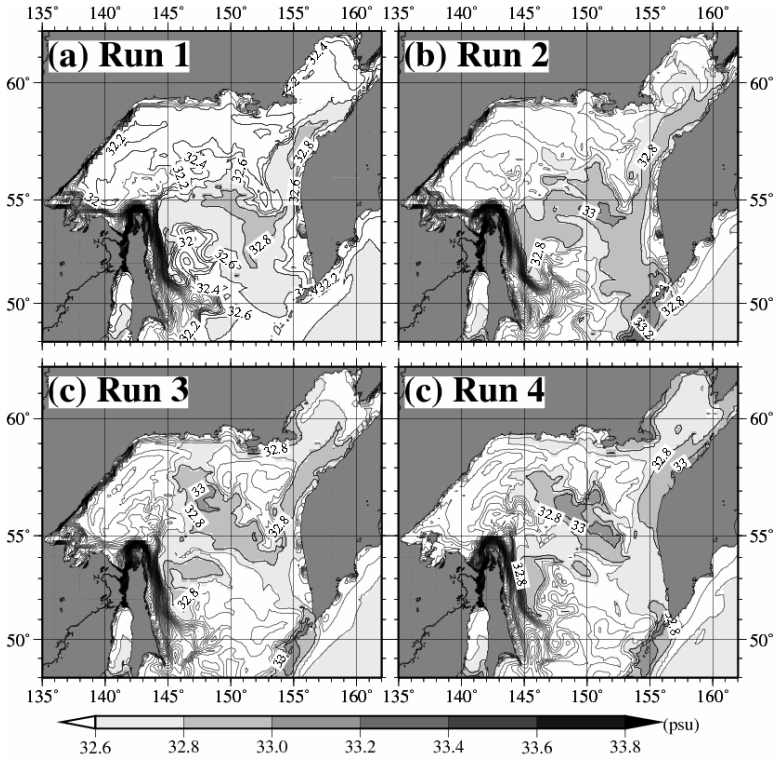

Fig. 4 Horizontal distributions of salinity in the top layer in September simulated in (a) Run 1, (b) Run 2, (c) Run 3 and (d) Run 4 (C.I. = 0.2 psu).

Martin *et al.*, 1998; Ohshima *et al.*, 2003). It can be considered that the more realistic the sea ice production results, the more brine rejection and DSW formation there is.

Abyssal density (Table 4) also increases by each effect. Horizontal distributions of abyssal density in September (Fig. 6) show that shaded regions where bottom water meets the criteria of the DSW in Itoh *et al.* (2003), increases by each effect. It corresponds to the increase of the DSW production rate. The observed distribution of abyssal density in September, 1999 around 56°N (thick solid line in Fig. 6a; Shcherbina *et al.*, 2003) shows a maximum near 140°E with density larger than 26.9 σ_θ. Such maxima of the abyssal density larger than 26.85 σ_θ are also shown on the same line in Run 3 and Run 4, in which the ECMWF wind stress is amplified by a factor of 1.5.

Annual mean SSS in the Okhotsk Sea (Table 5) mainly increases by adding the tidal effect (Run 2) and removing the river runoff (Run 4). SSS increases in all runs over the Okhotsk Sea by adding the tidal mixing effect (Fig. 4b). It seems that this increment is attributed to that of the northward salinity flux in the upper layer from the Kuril Islands originating with the upper salinity flux by the tidal mixing effect. The SSS intensification makes the brine in the northwestern shelf region more saline (denser) and results the more DSW formation, as mentioned in Nakamura *et al.* (2006). In Run 4 (Fig. 4d), the low-salinity front along the northwestern coast vanishes by removing the river runoffs in the Okhotsk Sea, except the Amur River. The increase of the abyssal density and the DSW formation may be attributed to the vanishing of the low-salinity front along the northwestern shelf region where the high production of sea ice and the brine rejection occurs.

Table 2 Annual mean DSW production rate (in Sv) in the northwestern shelf region.

Simulation	DSW prod. rate (Sv)
Run 1	0.14
Run 2	0.35
Run 3	0.48
Run 4	0.64
Nakamura *et al.* (2006)	0.13 (with the tidal effect)
Observational estimates	0.2–0.67

Note: The northwestern region is defined as the area north of 54°N and west of 153°E, with the bottom depth shallower than 200 m in this study.

Table 3 Annual sea ice production (in 10^{11} m^3) in the Okhotsk Sea.

Simulation	Ice production (10^{11} m^3)
Run 1	8.9
Run 2	9.4
Run 3	12.0
Run 4	12.2
Nakamura *et al.* (2006)	2.4 (With the tidal effect)
Ohshima *et al.* (2003)	13 (Observation)

Table 4 Annual mean abyssal density in the northwestern shelf region.

Simulation	Abyssal density (σ_θ)
Run 1	26.72
Run 2	26.80
Run 3	26.83
Run 4	26.88

Table 5 Annual mean sea surface salinity (SSS) in the Okhotsk Sea (in psu).

Simulation	SSS (psu)
Run 1	32.23
Run 2	32.37
Run 3	32.39
Run 4	32.60

SSS increases in the northern part of the Okhotsk Sea while it decreases in the southern part by the intensification of the wind stress in Run 3. The average SSS does not increase significantly in Run 3, (Table 5). It is considered that the wind-driven basin-scale circulation is intensified by the amplified wind in the Okhotsk Sea, and the salinity anomaly is transported farther north by the intensified circulation from the Kuril Islands, as mentioned in Matsuda (2008).

It seems there is one more effect of the amplified wind stress to the DSW formation. The annual sea ice production (Table 3) increases by intensification of the wind stress in Run 3 and Run 4. The northwestern coastal polynyas in Run 3 and Run 4 are wider and clearer than those in Run 1 and Run 2 because of intensification of the offshore wind along the northwestern coast. The horizontal distributions of annual sea ice production (Fig. 5) show a significant increment in sea ice production along the northwestern coast in Run 3 and Run 4. It is considered that the DSW formation is also intensified by the increase in brine rejection due to the intensification of the northwestern coastal polynya by the amplified wind.

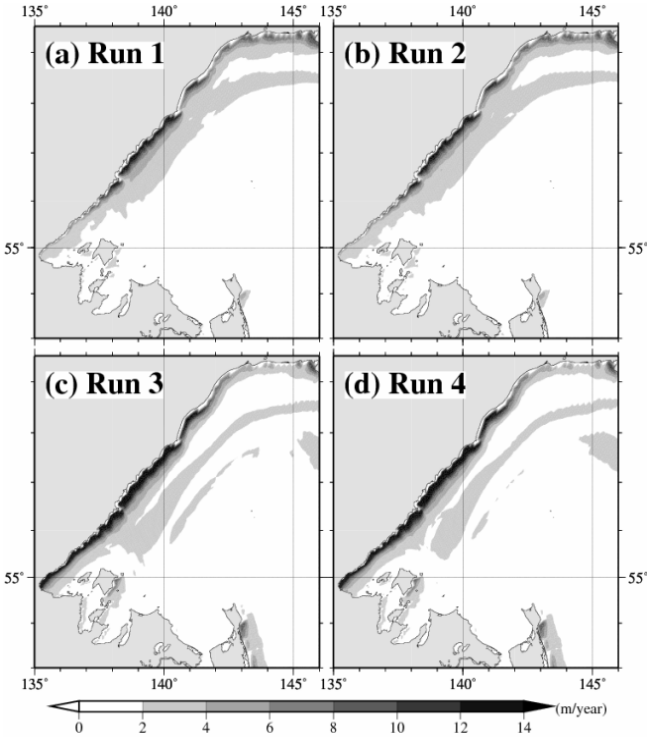

Fig. 5 Horizontal distributions of total annual sea ice production simulated in (a) Run 1, (b) Run 2, (c) Run 3 and (d) Run 4 (m $month^{-1}$).

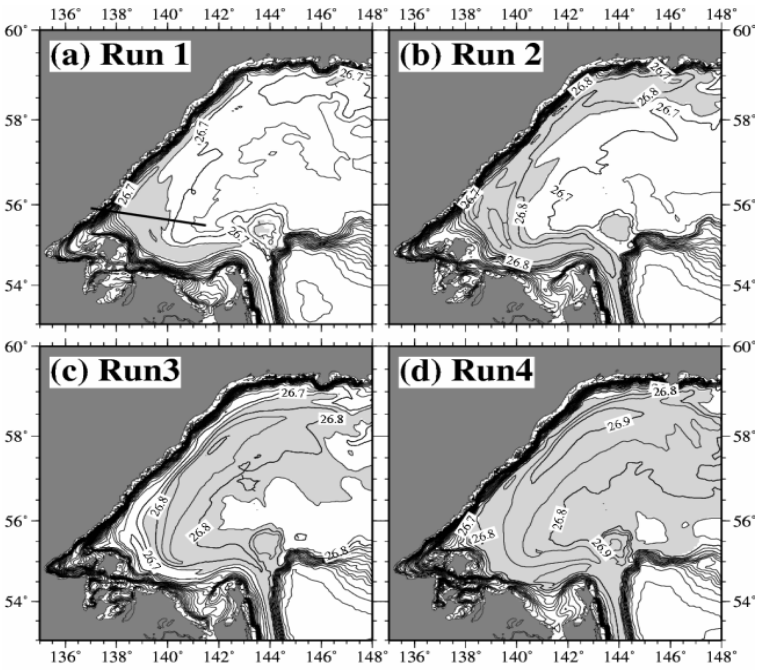

Fig. 6 Horizontal distributions of abyssal density around the northwestern shelf in September simulated in (a) Run 1, (b) Run 2, (c) Run 3 and (d) Run 4 (C.I. = 0.05 σ_θ). In shaded regions, abyssal density and temperature are larger than 26.75 σ_θ and colder than 0°C, respectively and match the DSW definition in Itoh *et al.* (2003). The solid line drawn at about 56°N in (a) indicates the observational line of Shcherbina *et al.* (2003).

Summary

In this study, the series of sensitivity experiments on the DSW formation in the Okhotsk Sea was performed with the sea–ice coupled model which well resolves the coastal polynya along the northwestern coast of the Okhotsk Sea.

The model reproduced more sea ice production and DSW formation than the former numerical studies because of the clearly reproduced northwestern coastal polynya. We confirmed the intensification of the DSW formation by the effects of tidal mixing in the Kuril Straits and the intensification of wind stress in the Okhotsk Sea, which makes the brine more saline in the northern shelf area, the same as in the former studies.

It was shown that the brine also becomes more saline by removing the unrealistically large amount of runoff in the Okhotsk Sea in the OMIP reanalysis dataset. On the other hand, Perry *et al.* (1996), which is used for validating the OMIP river runoff data, includes only runoffs of major rivers, and the accurate total amount of the river runoffs is currently not clear. Therefore, it cannot be said whether or not Run 4 reproduced more realistic DSW formation than Run 3 in the present study. We emphasize that there is a considerable amount of uncertainty in the river runoff datasets regarding DSW formation.

Sea ice production in the Okhotsk Sea increased because of the intensification of the wind stress in this study while it did not increase because of wind intensification in Matsuda (2008). This may be attributed to the reproduction of the clear coastal polynya because of the local high horizontal resolution of the model in this study. It is considered that the intensification of ice production due to wind intensification also contributes to the incremental amounts of brine and DSW production.

References

Alfultis, M.A. and Martin, S. 1987. Satellite passive microwave studies of the Sea of Okhotsk ice cover and its relation to oceanic processes, 1978−1982. *J. Geophys. Res.* **92**: 13,013−13,028.

Gladyshev, S., Martin, S., Riser, S. and Figurkin, A. 2000. Dense water production on the northern Okhotsk shelves – Comparison of ship-based spring-summer observations for 1996 and 1997 with satellite observations. *J. Geophys. Res.* **105**: 13,013−13,028.

Hasumi, H. 2006. CCSR Ocean Component Model (COCO) Version 4.0. CCSR report No. 25, 103 pp.

Itoh, M., Ohshima, K. and Wakatsuchi, M. 2003. Distribution and formation of Okhotsk Sea Intermediate Water: An analysis of isopycnal climatological data. *J. Geophys. Res.* **108**: doi:10.1029/2002JC001590.

Kara, A., Rochford, P. and Hurlburt, H. 2000. Efficient and accurate bulk parameterizations of air−sea fluxes for use in General Circulation Models. *J. Atmos. Ocean. Tech.* **17**: 1421−1438.

Kitani, K. 1973. An oceanographic study of the Okhotsk Sea. *Bull. Far Seas Fish. Res. Lab.* **9**: 45–77.

Martin, S., Drucker, R. and Yamashita, K. 1998, The production of ice and dense shelf water in the Okhotsk Sea polynyas. *J. Geophys. Res.* **103**: 27,771−27,782.

Matsuda, J. 2008. Numerical study of thermohaline circulation in the Sea of Okhotsk. M.Sc. thesis, 48 pp., Hokkaido Univ.

Mizuta, G., Fukamachi, Y., Ohshima, K.I. and Wakatsuchi, M. 2003. Structure and seasonal variability of the East Sakhalin Current. *J. Phys. Oceanogr.* **33**: 2430−2445.

Nakamura, T., Awaji, T., Hatayama, T., Akitomo, K., Takizawa, T., Kono, T., Kawasaki, Y. and Fukasawa, M. 2000. The generation of large-amplitude unsteady lee waves by subinertial K_1 tidal flow: a possible vertical mixing mechanism in the Kuril Straits. *J. Phys. Oceanogr.* **30**: 1601−1621.

Nakamura, T. and Awaji, T. 2004. Tidally induced diapycnal mixing in the Kuril Straits and its role in water transformation and transport: A three-dimensional nonhydrostatic model experiment. *J. Geophys. Res.* **109**: doi:10.1029/2003JC001850.

Nakamura, T., Toyoda, T., Ishikawa, Y. and Awaji, T. 2006. Enhanced ventilation in the Okhotsk Sea through tidal mixing at the Kuril Straits. *Deep-Sea Res. I* **53**: 425−448.

National Geophysical Data Center 1988. ETOPO−5 bathymetry/topography data. National Oceanic and Atmospheric Administration Data Announcement 88-MGG-02, U.S. Department of Commerce.

Ohshima, K.I., Wakatsuchi, M., Fukamachi, Y. and Mizuta, G. 2002. Near-surface circulation and tidal currents of the Okhotsk Sea observed with the satellite-tracked drifters. *J. Geophys. Res.* **107**: doi:10.1029/2001JC001005.

Ohshima, K., Watanabe, T. and Nihashi, S. 2003. Surface heat budget of the Sea of Okhotsk during 1987–2001 and the role of sea ice on it. *J. Meteorol. Soc. Jpn.* **81**: 653−677.

Ohshima, K.I., Simizu, D., Itoh, M., Mizuta, G., Fukamachi, Y., Riser, S.C. and Wakatsuchi, M. 2004. Sverdrup balance and the cyclonic gyre in the Sea of Okhotsk. *J. Phys. Oceanogr.* **34**: 513−525.

Ono, J., Ohshima, K.I., Mizuta, G., Fukamachi, Y. and Wakatsuchi, M. 2006. Amplification of diurnal tides over Kashevarov Bank in the Sea of Okhotsk and its impact on water mixing and sea ice. *Deep-Sea Res. I* **53**: 409–424.

Perry, G., Duffy, P. and Miller, N. 1996. An extended data set of river discharges for validation of general circulation models. *J. Geophys. Res.* **101**: 21,339−21,349.

Röske, F. 2001. An atlas of surface fluxes based on the ECMWF Re-analysis: A climatological dataset to force global ocean general circulation models. Max-Planck-Institut für Meteorologie Report 323, Max-Planck-Institute for Meteorology, p. 261.

Shcherbina, A., Talley, L. and Rudnick, D. 2003. Direct observations of North Pacific ventilation: Brine rejection in the Okhotsk Sea. *Science* **302**: 1952−1955.

Simizu, D. and Ohshima, K.I. 2002. Barotropic response of the Sea of Okhotsk to wind forcing. *J. Oceanogr.* **58**: 851−860.

Simizu, D. and Ohshima, K.I. 2006. A model simulation on the circulation in the Sea of Okhotsk and the East Sakhalin Current. *J. Geophys. Res.* **111**: doi:10.1029/2005JC002980.

Steele, M., Morley, R. and Ermold, W. 2001. PHC: A global ocean hydrography with a high-quality Arctic Ocean. *J. Climate* **14**: 2079−2087.

Takizawa, T. 1982. Characteristics of the Soya Warm Current in the Okhotsk Sea. *J. Oceanogr. Soc. Japan* **38**: 281−292.

Talley, L. 1991. An Okhotsk Sea water anomaly: implications for ventilation in the North Pacific. *Deep-Sea Res. A* **38**(Suppl. 1): S171−S190.

Tsujino, H., Hasumi, H. and Suginohara, N. 2000. Deep Pacific circulation controlled by vertical diffusivity at the lower thermocline depths. *J. Phys. Oceanogr.* **30**: 2853−2865.

Watanabe, T. and Wakatsuchi, M. 1998. Formation of 26. 8−26. 9 σ_θ water in the Kuril Basin of the Sea of Okhotsk as a possible origin of North Pacific Intermediate Water. *J. Geophys. Res.* **103**: 2849−2865.

Yasuda, I. 1997. The origin of the North Pacific Intermediate Water. *J. Geophys. Res.* **102**: 893−909.